MAGNETOHYDRODYNAMICS Vol. 45 (2009), No. 4, pp. 569–578

DRY CALIBRATION OF THE LORENTZ FORCE FLOWMETER

V. Minchenya, Ch. Karcher, Yu. Kolesnikov, A. Thess

Institute of Thermodynamics and Fluid Mechanics, Ilmenau University of Technology
PO Box 10 05 65, D-98684 Ilmenau, Germany

Lorentz force velocimetry is a technique for non-contact measurement of the flow rate in electrically conducting fluids like high-temperature liquid metal alloys. Before application, a proper calibration of the flowmeter is necessary. However, it is difficult to reproduce conditions typical of application in a laboratory environment. Therefore, we propose a simplified method, in which the working fluid is replaced by an electrically conducting moving solid, a method of dry calibration. It allows us to evaluate the basic uncertainties of the Lorentz force flowmeter (LFF) without the influence of the liquid flow dynamics. This is an introductory work presenting the main concept of the dry calibration of Lorentz force flowmeters.

Introduction. When a liquid of electric conductivity σ flows at a mean velocity $\mathbf{u}$ into an externally applied stationary magnetic field $\mathbf{B}$, eddy currents $\mathbf{j}$ are induced within the liquid. As a result of the interaction of these currents and the applied field, Lorentz forces $\mathbf{F}_\mathrm{L}$ are generated. The Lorentz forces tend to brake the flow. This well known electromagnetic braking effect is described by the equations of magnetohydrodynamics (Ohm's law and Lorentz force equation):

$$\mathbf{j} = \sigma\left(\mathbf{E} + \mathbf{v} \times \mathbf{B}\right), \qquad \mathbf{f}_\mathrm{L} = \mathbf{j} \times \mathbf{B}. \tag{1}$$

Here, $\mathbf{E}$ is the electric field and $\mathbf{f}_\mathrm{L}$ is the Lorentz force density. The resulting Lorentz force can be obtained by integrating the Lorentz force density over the interaction volume:

$$\mathbf{F}_\mathrm{L} = \int_V \mathbf{f}_\mathrm{L}\ \mathrm{d}V. \tag{2}$$

Combining equations (1) and (2) it is easy to show that the Lorentz force scales as

$$F_\mathrm{L} \sim \sigma B^2 \dot{V} L. \tag{3}$$

Here $\dot{V}$ is the volumetric flow rate (which we wish to measure) and L is a characteristic length scale, over which the magnetic field interacts with the fluid. The flow rate can be written as $\dot{V} = uS$, where u is the mean longitudinal velocity and S is the cross-section of the flow, as shown in Fig. 1.

In turn, by the Newton's 3rd law, the moving liquid exerts a counter force of equal strength on the system that generates the magnetic field, such as, for instance, an arrangement of permanent magnets [1]. Lorentz force velocimetry is based on measuring this counterforce, which by virtue of equation (3) is proportional to the flow rate of the liquid. The goal of the present paper is to investigate the practical applicability of equation (3) as well as to define the uncertainty of measurement in dry calibration.

The physical background of Lorentz force velocimetry is presented in more detail in [2–4]. Particularly, two different realizations of the LFF were considered, namely, a rotary flowmeter and a static flowmeter. The experimental results of

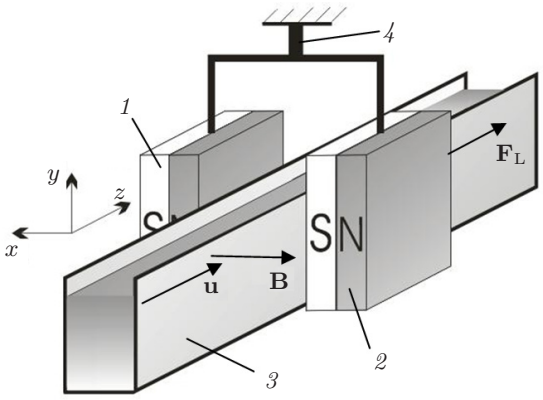

Fig. 1. Lorentz force flowmeter design. *1*, *2* – magnetic system; *3* – liquid metal flow (an open channel case is shown); *4* – force sensor.

measuring by the mentioned LFF devices were presented. It is shown experimentally in [3] that for the pipe flow the measured Lorentz force is in linear relation with the mean velocity of the flow. It is so because the magnetic Reynolds number is relatively small in our case ($\mathrm{Rm} = 0.05 \ldots 0.5$). Physically, this implies that the primary magnetic field is not distorted by the secondary one, generated by the eddy currents. Hence, the force sensor signal should be proportional to the longitudinal component of the mean velocity of the liquid melt flow [1]. It is shown that the LFF is suitable for the measurement of the volumetric flow rate.

The present study is organized as follows: in Section 1 we present the dry calibration equipment and the mathematical model. In Section 2 we present the results of the calibration procedure in the form of uncertainty budgets for all the major input and output parameters of the mathematical model. Finally, Section 3 provides the main conclusions.

1. Equipment and mathematical model of LFF dry calibration. In the present paper, we consider the Lorentz force flowmeter from the metrological point of view. In order to apply Lorentz force velocimetry to metallurgical processes like the production of secondary aluminum and steel casting, calibration of such flowmeters is necessary. Since it is often difficult or even impossible to calibrate a Lorentz force flowmeter (LFF) in a laboratory using the working fluid, we propose a simplified calibration method, a dry calibration, in which the working fluid is replaced by an electrically conducting moving solid (Fig. 2). During the

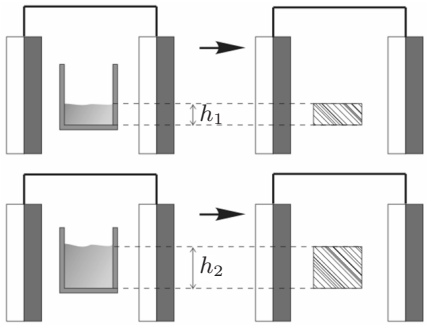

Fig. 2. The principle of replacement of the liquid metal open channel flow of different height by solid bodies (the flow direction and the bar displacement direction in the paper.

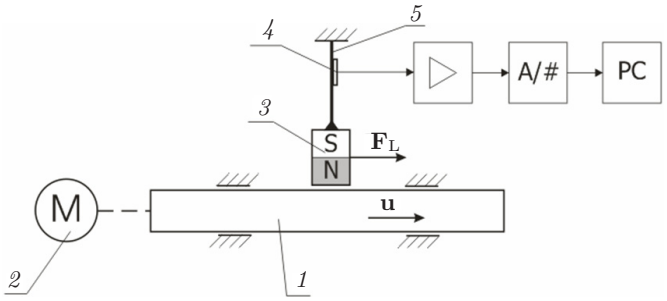

Fig. 3. Scheme of the dry calibration equipment for the Lorentz force flowmeter.

dry calibration procedure, the liquid metal flow is replaced by reference metal bars moving at a prescribed speed through the LFF magnetic system. This approach has the advantage that the velocity field is accurately known and the effects of turbulent velocity fluctuations are absent.

The LFF design principle is shown in Fig. 1. The external static magnetic field is generated by two sets of permanent magnets (pos. *1*, *2* in Fig. 1). The liquid metal flows in a channel (pos. *3*) and interacts with the applied magnetic field. The channel is situated within the magnetic system. The Lorentz force acting on the magnetic system is measured using a digital beam-type force sensor (pos. *4*).

The scheme of the LFF dry calibration experiment is presented in Fig. 3. The Lorentz force flowmeter, as given above, consists of a magnetic system (pos. *3*), a Lorentz force sensor (pos. *4*), and a bracket (pos. *5*) together with the data processing modules. During the dry calibration experiments, a solid metal reference bar (pos. *1*) is being moved through the magnetic system of the LFF along the flow direction. The signal from the force sensor is amplified and, after analog/digital conversion, transferred to the flow measurement software. In our case, the data processing module with operator interface is realized on the basis of LabView® package.

The pulling rate of the reference bar is controlled by a linear step motor (pos. *2*). Thus, in comparison with the real channel conditions, the velocity field of the flow is homogeneous and the cross-section is fixed (Fig. 4). Moreover, there are no velocity fluctuations due to the turbulence. Hence, the basic uncertainties of the LFF system can be accurately analyzed without being additionally influenced by the flow dynamics.

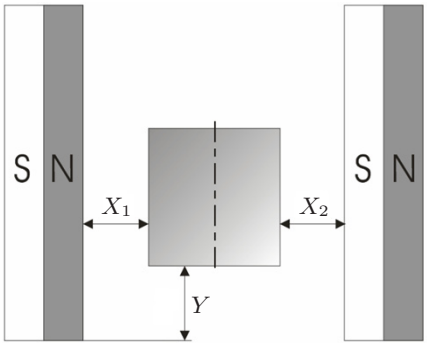

Fig. 4. Positioning of the cross-section of the reference bar within the magnetic system.

The location of the reference bar within the LFF magnetic system should be defined both in horizontal and in vertical coordinates (Fig. 4).

In our experiments, $X_1 = X_2$ and the parameter Y was always constant and equalled 30 mm. In application, this particular distance corresponds to the position of the bottom of the channel, within which the liquid metal flows. The length of the aluminum reference blocks was 1000 mm. The magnetic system consists of NeFeB magnet blocks with dimensions 100 mm×20 mm×20 mm, which are assembled to form two poles with a total pole area 140 mm×200 mm. The magnetization direction is across the flow. The magnets are mounted on a steel yoke, which has a Π-shape and closes the outer magnetic circuit. The distance between the poles is 250 mm. The mean induction of the stationary magnetic field in the area of location of the reference bar is 0.1 T.

At first, the response of the Lorentz force sensor to different loads applied to the magnetic system should be considered. The integral Lorentz force F_{L} is represented by the linear calibration characteristic of the force sensor:

$$F_{\mathrm{L}} = K_1 \cdot E_{\mathrm{i}}, \tag{4}$$

where E_{i} is the instant level of the sensor signal and K_1 is the calibration factor of the force sensor. Using equation (3), the measured instant velocity u of the reference bar can be represented by

$$u = \frac{K_2 \cdot F_{\mathrm{L}}}{\sigma}, \tag{5}$$

where K_2 is a calibration factor that incorporates characteristic geometry parameters and effective magnetic induction. Introduction of the coefficient K_2 is inevitable because it is not possible to separate variables B, S and L in equation (3). Equation (5) states that the measured Lorentz force is proportional to the velocity of the reference bar.

To investigate the behaviour of equation (5), a series of experiments was carried out, in which reference bars with different cross-sections were moved through the magnetic system at various velocities. The results of these experiments are presented in Fig. 5.

It can be seen from Fig. 5 that for a given constant cross-section of the reference bar the Lorentz force sensor signal linearly depends on the velocity of the reference bar. On the other hand, there is a highly nonlinear dependence of the Lorentz force sensor signal on the height of the reference bars at a given constant velocity. Hence, the linear equation (5) is valid for a single cross-section of the reference bar only.

From equations (4) and (5), we obtain the instant volumetric flow rate $\dot{V}$, which is given by

$$\dot{V} = uS = \frac{K_1 K_2 E_{\mathrm{i}}}{\sigma} S. \tag{6}$$

Equation (6) yields an invariant in relation to the reference bar velocity – a ratio of the Lorentz force to the volumetric flow rate $F_{\mathrm{L}}/\dot{V}$. This ratio must depend on the flow height h only. Hence, if our considerations are correct, then the functions $F_{\mathrm{L}}(h)/\dot{V}(h)$ at certain given velocities should lay on a single curve. On the other hand, for a given velocity the ratio should be constant in any given range of flow rates. The respective experimental diagrams in Fig. 6 prove these statements.

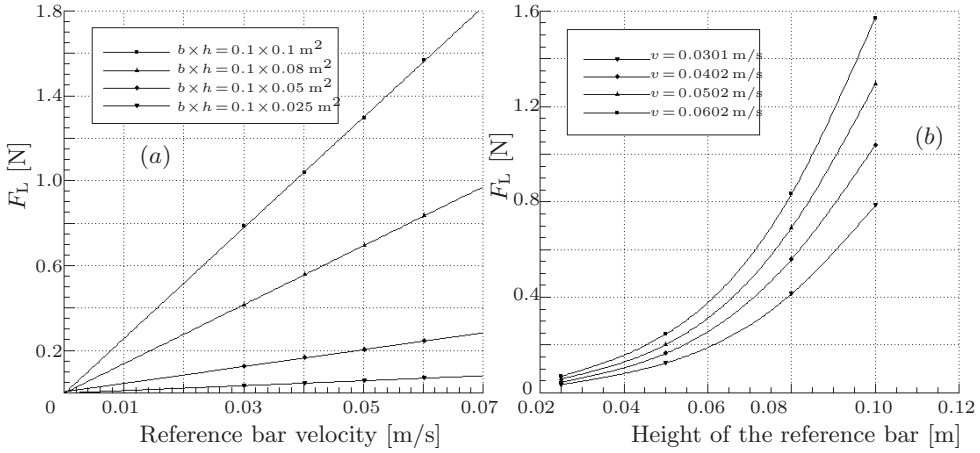

Fig. 5. Experimental results obtained at different velocities (a) with constant cross-sections of the reference bar, and (b) at constant velocities with different cross-sections of the reference bar. b and h are the width and the height of the reference bar, respectively.

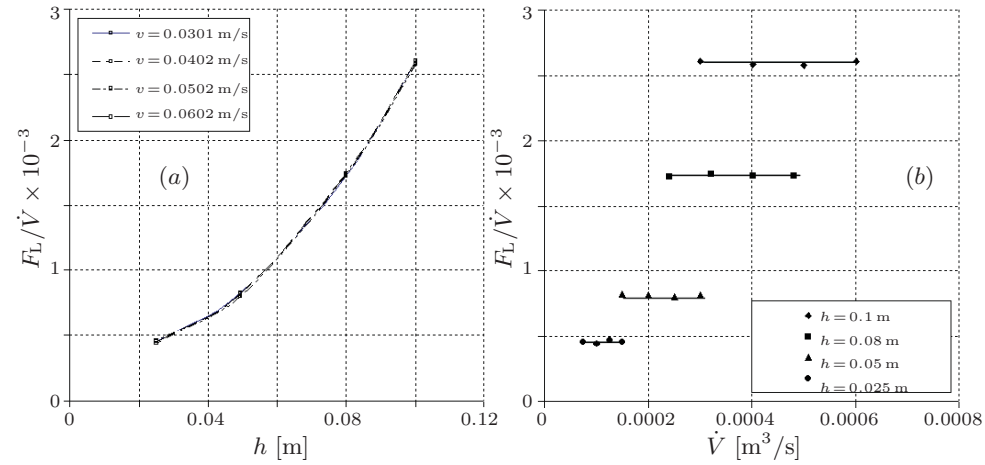

Fig. 6. The ratio of the measured Lorentz force to the volumetric flow rate (a) vs. the reference bar height and (b) vs. the volumetric flow rate.

2. Uncertainty budget of the LFF dry calibration. The dry calibration experiments were carried out on the LFF installation with the following basic characteristics:

1. Lorentz force sensor sensitivity 0.007 V/N;
2. Lorentz force measurement range 0. . . 9.7 N;
3. uncertainty of the sensor signal measurement ±0.0005 V.

The calibration factor K_1 is evaluated using equation (4). The relationship between the value of the static force applied in the direction of the reference bar motion and the amplitude of the sensor signal are determined. The load was applied using weights with uncertainty ±0.000025 N. The uncertainty budget for the parameter K_1 is presented in Table 1.

To evaluate the velocity of the reference bar, the actual displacement of the bar and the corresponding time period are measured using separate instruments. By that we obtain the actual precision of the linear step motor.

Table 1. Uncertainty budget of the parameter K_1.

Value X_i	Estimated value, x_i	Uncert. type	Probabil. distr.	Standart uncert. $u(x_i)$	Sens. coeff. c_i	Partial uncert., $u_{xi}(y)$
Init. level of output signal E_0, V	-0.0220	A	Norm.	0.0005	$0.1131\,\mathrm{NV}^{-2}$	$0.00006\ \mathrm{NV}^{-1}$
Maximal force applied $F_{\max}$, N	9.700000	B	Rect.	0.000025	$9.2593\,\mathrm{V}^{-1}$	$0.00023\ \mathrm{NV}^{-1}$
Sensor signal at maximal force $E_{\max}$, V	0.0860	A	Norm.	0.0005	$0.1131\,\mathrm{NV}^{-2}$	$0.00006\ \mathrm{NV}^{-1}$
Nonlinearity of the force sensor U_{NLS}, %	0.025					
The value of the parameter K_1, NV^{-1}	89.8			0.6		

Table 2. Uncertainty budget of the velocity u.

Value X_i	Estimated value, x_i	Uncert. type	Probabil. distr.	Standart uncert. $u(x_i)$	Sens. coeff. c_i	Partial uncert., $u_{xi}(y)$
Measured length of the displacement L, m	0.9468	A	Normal	0.0005	$0.0636\ \mathrm{s}^{-1}$	0.00003 m/s
Measured time t, s	15.73	A	Normal	0.01	$0.0038\ \mathrm{ms}^{-2}$	$3.8{\cdot}10^{-5}$ m/s
The value of velocity u, m/s	0.06020			0.00005		

Table 3. Uncertainty budget of the electric conductivity σ.

Value X_i	Estimated value, x_i	Uncert. type	Probabil. distr.	Standart uncert. $u(x_i)$	Sens. coeff. c_i	Partial uncert., $u_{xi}(y)$
The value of the electric conductivity σ, $\mathrm{S{\cdot}m}^{-1}$	2730			25		

Table 4. Uncertainty budget of the parameter K_2.

Value X_i	Estimated value, x_i	Standart uncert. $u(x_i)$	Sens. coeff. c_i	Partial uncert., $u_{xi}(y)$
The value of the parameter K_1, NV^{-1}	89.8	0.6	0.236 $\mathrm{SV\ s^{-1}N^{-2}}$	0.1416 $\mathrm{S\,s^{-1}N^{-1}}$
The value of velocity u, m/s	0.0602	0.0006	281.49 $\mathrm{Sm^{-1}N^{-1}}$	0.1689 $\mathrm{S\,s^{-1}N^{-1}}$
Sensor signal at maximal force $E_{i\max}$, V	0.0860	0.0005	196.261 $\mathrm{SV^{-1}s^{-1}N^{-1}}$	0.0981 $\mathrm{S\,s^{-1}N^{-1}}$
Init. level of output signal E_{i0}, V	–0.0220	0.0005	196.261 $\mathrm{SV^{-1}s^{-1}N^{-1}}$	0.0981 $\mathrm{S\,s^{-1}N^{-1}}$
The value of the electrical conductivity σ), $\mathrm{S\,m^{-1}}$	2730	25	0.0078 $\mathrm{mS^{-1}N^{-1}}$	0.1950 $\mathrm{S\,s^{-1}N^{-1}}$
The value of the parameter K_2, $\mathrm{S\,s^{-1}N^{-1}}$	21.196	0.325		

Table 5. Uncertainty budget of the cross-sectional area S.

Value X_i	Estimated value, x_i	Uncert. type	Probabil. distr.	Standart uncert. $u(x_i)$	Sens. coeff. c_i	Partial uncert., $u_{xi}(y)$
Variation of height h and width b with length U_{LR}, m	0.00025					
Reference bar width b, m	0.01	B	Rect.	0.00027	0.01	$2.7 \cdot 10^{-6}$ $\mathrm{m^2}$
Reference bar height h, m	0.01	B	Rect.	0.00027	0.01	$2.7 \cdot 10^{-6}$ $\mathrm{m^2}$
The value of the cross-sectional area S, $\mathrm{m^2}$	0.000100			0.000004		

Table 6. Uncertainty budget of the volumetric flow rate $\dot{V}$.

Value X_i	Estimated value, x_i	Uncert. type	Probabil. distr.	Standart uncert. $u(x_i)$	Sens. coeff. c_i	Partial uncert., $u_{xi}(y)$
Calibration factor K_1, NV^{-1}	89.8			0.6	$1.1 \cdot 10^{-8}$ $\mathrm{Vm^3s^{-1}N^{-1}}$	$6.6 \cdot 10^{-9}$ $\mathrm{m^3s^{-1}}$
Calibration factor K_2, $\mathrm{S\,s^{-1}N^{-1}}$	21.196			0.325	$4.3 \cdot 10^{-8}$ $\mathrm{Nm^3S^{-1}}$	$1.4 \cdot 10^{-8}$ $\mathrm{m^3s^{-1}}$
Force sensor signal E_i, V	0.0130	A	Rect.	0.0001	$6.9 \cdot 10^{-5}$ $\mathrm{m^3s^{-1}V}$	$6.9 \cdot 10^{-9}$ $\mathrm{m^3s^{-1}}$
Cross-sectional area S, $\mathrm{m^2}$	0.000100			$4 \cdot 10^{-6}$	0.00007 $\mathrm{ms^{-1}}$	$2.8 \cdot 10^{-10}$ $\mathrm{m^3s^{-1}}$
Electric conductivity σ, $\mathrm{Sm^{-1}}$	2730			25	$3.32 \cdot 10^{-10}$ $\mathrm{m^4s^{-1}S^{-1}}$	$8.3 \cdot 10^{-9}$ $\mathrm{m^3s^{-1}}$
The value of the measured volumetric flow rate $\dot{V}$ $\mathrm{m^3s^{-1}}$	$9.0 \cdot 10^{-7}$			$1.8 \cdot 10^{-8}$		

The displacement was measured using the laser distance sensor with nominal uncertainty of measurement $\pm 0.00025\,\mathrm{m}$.

Time was measured using an electronic timer with nominal uncertainty of measurement $\pm 0.005\,\mathrm{s}$. Start and stop functions of the timer were synchronized with the linear guide of the calibration equipment using electro-contact sensors. The uncertainty budget for the velocity u is presented in Table 2.

The value of the electric conductivity of the reference aluminum bars and the uncertainty of its evaluation are given by the supplier of the bars (Table 3). The authors have no possibility to measure the conductivity *in situ* at the moment, though this question is to be emphasized in the future, because the conductivity shows a strong dependence on the temperature, for instance, [5].

The calibration factor K_2 is evaluated on the basis of equation (5). The value of the parameter is valid for a given cross-section of the reference bar. The reference bar is moved within the magnetic system with a given velocity u. The measured signal of the Lorentz force sensor is a primary measurement data in this experiment.

The uncertainty budget of the calibration factor K_2 for the case of the reference bar with the height $h = 100\,\mathrm{mm}$ and width $b = 100\,\mathrm{mm}$ is given in Table 4. The uncertainty budget for the reference bar cross-section is presented in Table 5.

The volumetric flow rate is the primary measurement value of the Lorentz force flowmeter. The volumetric flow rate is evaluated using the calibration data considered above. The uncertainty budget for the volumetric flow rate is given in Table 6.

The uncertainty achieved in the presented study (2%) is exemplary. The practical uncertainty reachable in dry calibration experiments with solid metal bars can be as low as 0.5% and even lower.

3. Conclusion. In this article, the concept of the dry calibration of Lorentz force flowmeters using solid aluminium bars is reported. We present a mathematical model of calibration allowing us to evaluate the relevant calibration factors and to give estimates of the measurement uncertainties. The uncertainty budgets (in agreement with ISO 17025 standard [6]) for all input and output values of the mathematical model are presented. The budgets are presented in separate tables to keep the structure of the resulting LKA uncertainty clear.

For precise measurement in metallurgical applications, extended calibration measurement within the procedure of liquid calibration is necessary to account for the inhomogeneous velocity field. Integration of the dry calibration technique in the whole structure of the LFF calibration for open channels will be considered in further publications.

Acknowledgements. The authors gratefully appreciate the support of Bundesministerium für Bildung und Forschung within the framework of project 03FO1291. We are grateful to our technicians Eckhard Roth and Vigimantas Mitschunas, who have made much effort to make this research technically possible. We also acknowledge the help of Javier Fiasche and Marek Stefansson, who performed some calibration measurements in the course of their project works.

REFERENCES

[1] P. Davidson. *An Introduction to Magnetohydrodynamics* (Cambridge: Cambridge University Press, 2001).

[2] J. Shercliff. *A Textbook of Magnetohydrodynamics* (London: Longman, 1965).

[3] A. Thess, E. Votyakov, Y. Kolesnikov. Lorentz force velocimetry. *Physical Review Letters*, vol. 96 (2006), 164501-1-4.

[4] A. Thess, Y. Kolesnikov, Ch. Karcher, E. Votyakov. Lorentz force velocimetry – a contactless technique for flow measurement in high-temperature melts. In *Proc. 5th International Symposium on Electromagnetic Processing of Materials* (Sendai, Japan, 2006).

[5] R. Brandt , G. Neuer. Electrical resistivity and thermal conductivity of pure aluminium and aluminium alloys. *Int. J. Thermophys.*, vol. 28 (2007), pp. 1429–1446.

[6] European Co-operation for Accreditation. Expression of the Uncertainty of Measurement in Calibration. EA-4/02, 79 (1999).

Received 15.10.2009